

Pulmonary toxicity of instilled cadmium-doped silica nanoparticles during acute and subacute stages in rats

Teresa Coccini¹, Sergio Barni², Rita Vaccarone², Piercarlo Mustarelli³, Luigi Manzo^{1,4} and Elisa Roda¹

¹Salvatore Maugeri Foundation IRCCS, Toxicology Division, ²Department of Animal Biology, Comparative Anatomy Division,

³Department of Physical Chemistry and ⁴Department of Internal Medicine and Therapeutics, University of Pavia, Pavia, Italy

Summary. Potential risk associated with new nanomaterial exposure needs to be assessed. This *in vivo* study investigated pulmonary effects of engineered cadmium-containing silica nanoparticles Cd/SiNPs (1 mg/rat), silica SiNPs (600 µg/rat) and CdCl₂ (400 µg/rat) 1, 7 and 30 days after intratracheal instillation. Comprehensive histopathological and immunocytochemical characterization of lung damage in terms of apoptosis, cell proliferation, inflammation, fibrosis and metabolism were obtained.

After exposure to all treatments, lung parenchyma showed injury patterns characterized by collapsed alveoli, inflammation, granuloma formation, thickened alveolar septa and bronchiolar epithelium exfoliation. Type II pneumocytes, containing scarcely surfactant-lamellated bodies, were also observed. Apoptotic phenomena enhanced as following, Cd/SiNPs>CdCl₂>SiNPs. In parallel with these findings, a significant increase of PCNA-immunoreactive cells was detected together with high mitotic activity. Cellular localization and distribution of IL-6, IP-10 and TGF-β1 revealed an increased expression of these cytokines as evidence of an enhanced cellular inflammatory response. CYP450-immunoreactivity was also enhanced, at bronchiolar (e.g. Clara cells) and alveolar (e.g. macrophages) level after both Cd/SiNPs and CdCl₂. These overall effects were observed acutely and lasted until the 30th day, with Cd/SiNPs producing the most marked effects.

Collagen-immunolabelling changed particularly 7 and 30 days after Cd/SiNPs, when a strong stromal fibrogenic reaction occurred.

The present findings suggest that Cd/SiNPs produce significantly greater pulmonary alterations than either SiNPs or CdCl₂ under the present experimental

conditions.

Key words: Nanotoxicology, *In vivo*, Apoptosis, Inflammation, Fibrosis

Introduction

In the latest decades growing worldwide attention has been devoted to engineered silica (SiO₂) nanoparticles (SiNPs) based on their putative novel applications in a variety of industries, including biomedical and biotechnological fields (e.g., cancer therapy, DNA transfection, imaging, and controlled drug delivery) (Ravi Kumar et al., 2004; Bharali et al., 2005; Gemeinhart et al., 2005; Oberdörster et al., 2005; De Jong and Borm, 2008; Slowing et al., 2008).

A paucity of toxicity experimental data is available for amorphous and nano-size forms of silica, in contrast to the wide information existing on the well-studied crystalline micron-sized silica (Napierska et al., 2010).

Interestingly, nanoparticles possess novel properties, kinetics and unusual bioactivity, although their potential biological effects may not necessarily be easily predicted from previous studies of micron-size bulk materials.

Due to the unique physico-chemical properties of nano-sized silica, much concern has been expressed about the potential of adverse and unanticipated toxic effects on human health, including an enhanced ability to penetrate intracellular targets in the lung and through the systemic circulation (Donaldson et al., 2001; Maynard et al., 2006). For instance, ultrafine particles have been shown to cause development of particle-mediated lung diseases, including greater pulmonary inflammatory responses, than those induced by the fine particles per given mass (Li et al., 1999; Nemmar et al., 2003; Zhang et al., 2003). Also, experiments using silica nanoparticles, both in amorphous colloidal (Kaewamatawong

et al., 2005; Wang et al., 2007) and crystalline (Wang et al., 2007) forms, have demonstrated their greater ability to cause lung injury as compared with fine particles. Thus, the unique properties (i.e., small size and corresponding large specific surface area; cell penetrating ability) of nano-sized SiO_2 are likely to impose biological effects that differ greatly from micron-scale counterparts.

Crystalline silica is known to cause adverse health effects: for the micron-sized crystalline silica form, the most important mechanisms involved in the inflammogenic and fibrogenic activities (Fubini and Hubbard, 2003; Sayes et al., 2007) and/or carcinogenic activity (Saffiotti, 1992; IARC, 1997) seem to be oxidative stress and, linked to it, oxidative DNA and membrane damage. Whereas amorphous silica, being generally free of crystalline forms, is considered to be less toxic, and therefore it has been less studied. Findings indicate that synthetic amorphous silica is not involved in progressive fibrosis of the lung (Reuzel et al., 1991; Lee and Kelly, 1992); however, high doses of amorphous silica may result in acute pulmonary inflammatory responses (Rosenbruch, 1992). Amorphous silica in the form of engineered SiNPs have been increasingly used for different applications. However, although only limited *in vivo* studies on SiNPs are available, findings have reported that they can cause adverse health effects depending on their manufacturing process and the current data do not clarify whether amorphous SiNPs – showing cytotoxicity via oxidative stress, pulmonary inflammation, induction of expression of matrix metalloproteinases, and transient fibrosis (Kaewamatawong et al., 2006; Choi et al., 2008; Park et al., 2011) – are less or more harmful as compared with micron-sized silica.

In addition, SiNPs may contain metals as contaminants, but the enhancing effects of metals on NP toxicity, and whether or not these NPs can act as carriers of toxic metals, is still unknown (Maynard et al., 2006). On the other hand, silica NPs incorporating cadmium have been developed for potential application in informatics and as drug delivery devices (Barik et al., 2008; Rzigelinski and Strobl, 2009; Vivero-Escoto et al., 2010). Fluorescent, radio-opaque, and paramagnetic CdS-containing “quantum dots” have been produced as a multifunctional probe for bioimaging.

Cadmium (Cd) is a highly reactive metal, and its chief route of exposure is via the respiratory system (Oberdörster et al., 1992, 1994; Potts et al., 2001). Because of its stability in the environment and long retention time in the human body (half-life, ~ 20 years), Cd can accumulate and cause a variety of adverse effects (Waalkes, 2003; Joseph, 2009). The target organs for Cd toxicity include the liver, kidney, lung, testis, prostate, and bladder. However, prolonged human exposure to Cd results mainly in diseases affecting lungs and kidneys (IARC, 1993; ATSDR, 2008). Inhalation of Cd can result in acute injury such as oedema, or under chronic exposure these changes can progress to emphysema,

pulmonary fibrosis or adenocarcinomas.

Since nanoparticles have unique physicochemical properties and functionalities that are different from their bulk counterparts, their mode of action may vary greatly based on their physicochemical parameters. It is therefore crucial to determine the appropriate way to compare physicochemical properties with fate and toxicity.

The approach taken in this study was to evaluate the *in vivo* effects of engineered NPs (ENPs), namely silica NPs doped with Cd (Cd/SiNPs) compared to the effects produced by the “SiNPs” counterpart (not doped) on lung tissues (portal organ of entry). Cadmium, a well recognized pneumotoxicant, was used as a tool and employed in the dosage and chemical form known to induce lung toxicity in rodents. The dose selected and the mode of exposure were based on previous experiments showing lung dysfunction, cytotoxicity, edema and fibrosis after intra-tracheal (i.t.) instillation of cadmium chloride (Damiano et al., 1990; Bell et al., 1997, 2000). In particular, lung injury induced by CdCl_2 given i.t. at the dose of $400 \mu\text{g}/\text{rat}$ ($=245 \mu\text{g Cd}$) was shown to represent a good model of human interstitial lung disease (Damiano et al., 1990).

The present investigation was focused on specific endpoints and pathological outcomes of the pulmonary tissue. In particular, the evaluated morphological and molecular effects included: (i) histopathology of lung tissue (by means of Haematoxylin/Eosin Staining and TEM analysis), (ii) characterization of apoptotic/proliferating features by TUNEL and PCNA immunostaining, and (iii) immunohistochemical evaluation of the presence/distribution of (1) TGF- $\beta 1$ (Transforming Growth Factor-beta1), (2) IL-6 (Interleukin-6), IP-10 (interferon-gamma-induced protein), Eotaxin, (3) Collagen (Type I), and (4) cytochrome P450, (5) calmodulin. These endpoints were assessed as markers of general lung toxicity, inflammation, fibrosis, and metabolism, respectively.

Comparative data assessment was analyzed in terms of the biological responses to the three types of treatment in relation to persistence, delay, or tendency to resolution of these effects by considering the evaluation at different time points, i.e. 24 h, 7 and 30 days post-exposure.

Materials and methods

Preparation of NP of silica containing Cd salt

Impregnation of SiO_2 (silica nanosize HiSil™ T700 commercial Degussa GmbH - Germany, average pore size 20 nm, surface area $240 \text{ m}^2/\text{g}$, pore specific volume of $0.4 \text{ cm}^3 \text{ g}^{-1}$; HiSil™ T700 also contains 8-10 hydroxyl groups per nm^2 of surface) with cadmium nitrate hydrate was obtained from a preparation of aqueous solution of CdNO_3 $3.56 \times 10^{-2} \text{ M}$, in which the silica was dispersed in concentration ratio which produces a sample containing 40% Cd by weight.

Dispersion was brought to dryness and treated at 600°C for 2 hr in air. This heat treatment leads to the decomposition of nitrate Cd to Cd oxide, dispersed in silica. Powder was later subjected to grinding mills with high energy (200 rpm for 1.5 hr, 400 rpm for 1.5 hr, 600 rpm for 2 hr) to get the most equal distribution of particle size and/or aggregates of particles. The thermal treatment followed by heating the particles at higher temperatures (about 500-600°C) was performed in order to remove the residual organic groups. The thermal processes have allowed also to remove possible endotoxin contamination (e.g. lypopolysaccharides) according to the Food and Drug Administration guidelines (Vallhov et al., 2006).

Attention was devoted to tune the thermal treatments in order to retain the grain dimensions, pore size, and distributions, and particle surface areas. The entire synthesis preparation was performed under sterile conditions (e.g. using laminar flow cabinet, ultrapure water, autoclaved glassware) to avoid NPs contamination. An endotoxin assay confirms the absence of detectable gram negative endotoxin on both NP types, namely SiNPs and Cd/SiNPs, at the concentration of 1 mg/ml (the detection limit was less than 0.1 EU/ml).

Cd concentration released from NP of silica in the physiological solution was determined by Flame-atomic absorption analysis for trace metals. Quantitative analysis was also performed on the Cd/SiNPs sample for the presence of trace metals.

Physicochemical characterization of Cd/SiNPs

Before *in vivo* exposure by intratracheal instillation (i.t.), exhaustive physicochemical characterization of Cd/SiNPs was performed by STEM (scanning transmission electron microscopy) technique: energy dispersion X-ray (EDX), X-ray powder (XRD) diffraction, and Dynamic light scattering (DLS).

Cd/SiNPs were imaged by STEM technique: energy dispersion X-ray (EDX) was used for point and line profile analysis. STEM with a large-angle annular dark-field (HAADF) was used to give Z-contrast profile (CAMSOR, University of Oregon, Eugene, OR, USA).

X-ray powder (XRD) diffraction was used to determine phase composition of the Cd/SiNPs. It was determined at room temperature on a Rigaku Ultima IV X-ray diffractometer with a CuK α source ($\lambda=1.5418\text{ \AA}$). Phase analysis for the sample was carried out based on the International Center for Diffraction Data (ICDD) database (PDF-2 support software, 2009).

Dynamic light scattering (Zetasizer Nano ZS90, Malvern Instruments, Alfatest-Roma Italy) was used to measure the size distribution of Cd/SiNPs and SiNPs (in deionized water) and their zeta potential.

In vivo study: Animals and treatments

Adult male Sprague-Dawley rats (12 weeks old) were purchased from Charles River Italia (Calco, Italy)

and allowed to acclimatize for at least 2 weeks prior to treatment. Animals were housed under constant conditions of temperature, humidity, and photocycle (12 h light/12 h dark) with unlimited access to a commercial rat diet (VRF1 Mucedola from Charles River Italia) and tap water.

The weight of rats in all treatment groups at the time point 0 (day of instillation) was g 278±3.

All experimental procedures involving animals were performed in compliance with the European Council Directive 86/609/EEC on the care and use of laboratory animals. All animals used in this research have been treated humanely according to the institutional guidelines, with due consideration for the alleviation of distress and discomfort.

For the treatment, groups of rats (n=6 total for each treatment group at each time point) were anesthetized with pentobarbital sodium for veterinary use and were i.t. instilled with Cadmium Chloride ($CdCl_2$), Silica NPs (SiNPs), and Cadmium-doped Silica NPs (Cd/SiNPs) (see section 2.1, 2.2), dispersed at a dose of 400 $\mu\text{g}/\text{rat}$, 600 $\mu\text{g}/\text{rat}$ and 1 mg/rat, respectively, in 100 μl NaCl 0.9%. Just before i.t. exposure, the different NP suspensions were prepared by vortexing the suspension on ice to further force NP dispersion, avoiding the tendency to agglomerate and the formation of aggregates. No surfactants or solvents were used. The suspensions of the test materials were immediately used for the treatment.

Twenty-four hours, 7 and 30 days after i.t., a set (n=3 animals for each treatment and at each time point) of treated and control rats were deeply anesthetized with an overdose i.p. injection of 35% chloral hydrate (100 $\mu\text{l}/100\text{ g b.w.}$); lung preparation for morphohistochemical evaluations was done by vascular perfusion of fixative. Briefly, the trachea was cannulated, and laparotomy was performed. The pulmonary artery was cannulated via the ventricle, and an outflow cannula was inserted into the left atrium. In quick succession, the tracheal cannula was connected to about 7 cm H_2O pressure source to inflate the lungs with air, and clearing solution (saline with 100 U/ml heparin, 350 mosM sucrose) was perfused via the pulmonary artery. After blood was cleared from the lungs, the perfusate was switched to fixative consisting of 4% paraformaldehyde in 0.1 M phosphate buffer (pH 7.4). After fixation, the lungs were carefully removed.

Tissue sampling

Lungs

The top and the bottom regions of the right lungs of control and differently treated animals were dissected. Tissue samples were obtained according to a stratified random sampling scheme which is a suggested method for lung tissue in order to compensate for regional differences which are known to exist in the lung (Weibel, 1979) and to reduce the variability of the

sampling means.

From each slice, 2-3 blocks were systematically derived, washed in NaCl 0.9% and post-fixed by immersion for 7 hr in 4% paraformaldehyde in 0.1 M phosphate buffer (pH 7.4), dehydrated through a graded series of ethanol and finally embedded in Paraplast. Eight μm thick sections of the samples were cut in the transversal plane and collected on silan-coated slides.

Histology and cytochemistry

Lung sections of control and treated rats were stained with Haematoxylin/Eosin (H&E) to evaluate overall tissue structural changes.

Immunocytochemistry

To avoid possible staining differences due to small changes in the procedure, the reactions were carried out simultaneously on slides of control and treated animals at all stages.

Immunocytochemistry was performed using commercial antibodies on rat lung specimens to assess (1) the presence and distribution of (i) TGF- β 1, (ii) IL-6, (iii) IP-10, (iv) Eotaxin, (v) Collagen (Type I) and (vi) Proliferating Cell Nuclear Antigen (PCNA-PC10), as typical markers of general lung toxicity, inflammation, fibrosis, and cell proliferation/DNA repair, respectively; and (2) the presence and alteration of (i) Cytochrome P450, and (ii) calmodulin.

Lung sections of control and treated rats were incubated overnight at room temperature with: (i) a primary rabbit polyclonal antibody against TGF- β 1 (Santa Cruz Biotechnology, Santa Cruz, CA, USA) diluted 1:100 or (ii) a primary rabbit polyclonal antibody against Collagen (Type I) (Chemicon, Temecula, CA, USA) diluted 1:400 or (iii) a primary goat polyclonal antibody against IL-6 (Santa Cruz Biotechnology) diluted 1:100 or (iv) a primary mouse monoclonal antibody against PCNA-PC10 (American Biotechnology, Plantation, USA) diluted 1:5 or (v) a primary rabbit polyclonal antibody against Cytochrome P450 (Chemicon, Temecula, CA, USA), diluted 1:300, or (vi) a primary rabbit polyclonal antibody against calmodulin (Swant, Bellinzona, Switzerland) diluted 1:1000, or (vii) a primary goat polyclonal antibody against IP-10 (Santa Cruz Biotechnology, Santa Cruz, CA, USA) diluted 1:200, or (viii) a primary goat polyclonal antibody against Eotaxin (Santa Cruz Biotechnology, Santa Cruz, CA, USA) diluted 1:200; all the above mentioned antibodies were diluted in PBS.

Biotinylated anti-rabbit, anti-goat and anti-mouse secondary antibodies and an avidin biotinylated horseradish peroxidase complex (Vector Laboratories, Burlingame, CA, USA) were used to reveal the sites of antigen/antibody interaction. The 3,3'-diaminobenzidine tetrahydrochloride peroxidase substrate (Sigma, St. Louis, MO, USA) was used as chromogen, and

Haematoxylin was employed in some specimens for nuclear counterstaining. Then, the sections were dehydrated in ethanol, cleared in xylene, and finally mounted in Eukitt (Kindler, Freiburg, Germany).

As negative controls, some sections were incubated with phosphate-buffer saline in absence of the primary antibodies; no immunoreactivity was observed in this condition.

TUNEL staining

In addition to morphological criteria, apoptotic cell death was assayed by *in situ* detection of DNA fragmentation using the terminal deoxynucleotidyl-transferase (TUNEL) assay (Oncogene Res. Prod., Boston, MA, USA). The lung sections were incubated for 5 min with 20 μg ml⁻¹ proteinase-K solution at room temperature, followed by treatment with 3% H₂O₂ to quench endogenous peroxidase activity. After incubation with the TUNEL solution (90 min with TdT/biotinylated dNTP and 30 min with HRP-conjugate streptavidin) in a humidified chamber at 37°C, the reaction was developed using 0.05% 3-amino-9-ethylcarbazole (AEC) in 0.1 M TRIS buffer (pH 7.6) with 0.2% H₂O₂; in some specimens the reaction was developed using a 0.1% DAB solution. The specimens were lightly counterstained with Haematoxylin.

As a negative control, in some sections the TdT incubation was omitted; no staining was observed in these conditions.

Cytochemical assessment

(i) Scoring different specimens, the immunostaining for IL-6, TGF- β 1, IP-10, Eotaxin, Calmodulin, CYP450, Collagen (Type I) was evaluated in conventional brightfield microscopy by recording the localization and intensity of labelling according to a semiquantitative scale from absent/undetectable (-) to maximal (++)+. Then, to assess the significance of the immunohistochemical results, a Kruskal-Wallis non-parametric analysis of the semiquantitative data was performed. A p value of <0.05 was considered significant.

(ii) The evaluation of PCNA- and TUNEL-cytochemically positive cells (PCNA L.I., TUNEL L.I.) was calculated as the percentage (Labelling Index) of a total number (about 500) of all cells (bronchiolar, alveolar and stromal of the lung parenchyma), for each animal and experimental condition, in a minimum of 10 randomly selected high-power microscopic fields. Statistical analyses among the different biological situations was performed by two-way analysis of variance (ANOVA) followed by the Bonferroni test.

The slides were observed and scored with a bright-field Zeiss Axioscop Plus microscope. The images were recorded with an Olympus Camedia C-2000 Z digital camera and stored on a PC running Olympus software.

Electron microscopy

Lung fragments (small blocks of about 1 mm³) from a second set of rats (n=3 for each treatment at each time point) were fixed for 4 hrs by immersion in icecold 1.5% glutaraldehyde (Polysciences, Inc. Warrington, PA, USA) buffered with 0.07 M cacodylate buffer (pH 7.4), containing 7% sucrose, followed by post-fixation in OsO₄ (Sigma Chemical Co., St. Louis, MO, USA) in 0.1 M cacodylate buffer (pH 7.4) for 2 hr at 4°C, dehydrated in a graded series of ethanol and embedded in Epon 812. Semithin sections (1 μ m thick) were stained with 1% borated methylene blue. Ultrathin sections (about 600 \AA thick) were cut from the blocks, mounted on uncoated 200-mesh-copper grids, and doubly stained with saturated uranyl acetate in 50% acetone and Reynold's lead citrate solution. The specimens were examined with a Zeiss EM 300 electron microscope operating at 80 kV.

Statistical analysis

For histology and immunocytochemistry: TUNEL and PCNA data were analyzed by two-way analysis of variance (ANOVA) followed by the bonferroni test for

multiple mean comparison. Differential immunolabeling expression data are not normally distributed so the Kruskal-Wallis nonparametric test was used. Statistical significance is indicated with a * (P value <0.05). In all graphs error bars represent the standard deviation of the mean.

Results

Evaluation of the release time of Cd from silica nanoparticles (Cd/SiNPs)

Cd concentration released from NP of silica in the physiological solution was linear during a period of 16-232 hr (evaluated by linear regression: $y = 473.24 + 0.7235x$, $R^2 = 0.9975$). The maximum release (about 15%) was observed after 16 hr in physiological solution.

Purity of NP doped with cadmium

Quantitative analysis was performed on the Cd/SiNPs, to verify the amount of doping effectively dispersed in the silica and the presence of any metal

Qualitative analysis results

Phase name	Formula	Figure of merit	Phase reg. detail	DB card number
Cadmium Nitrate	Cd(OH)N O3 - H2O	0.671	ICDD (PDF2009)	00-018-0260
Silicon Oxide	Si O2	1.142	ICDD (PDF2009)	00-029-0085

Phase data pattern

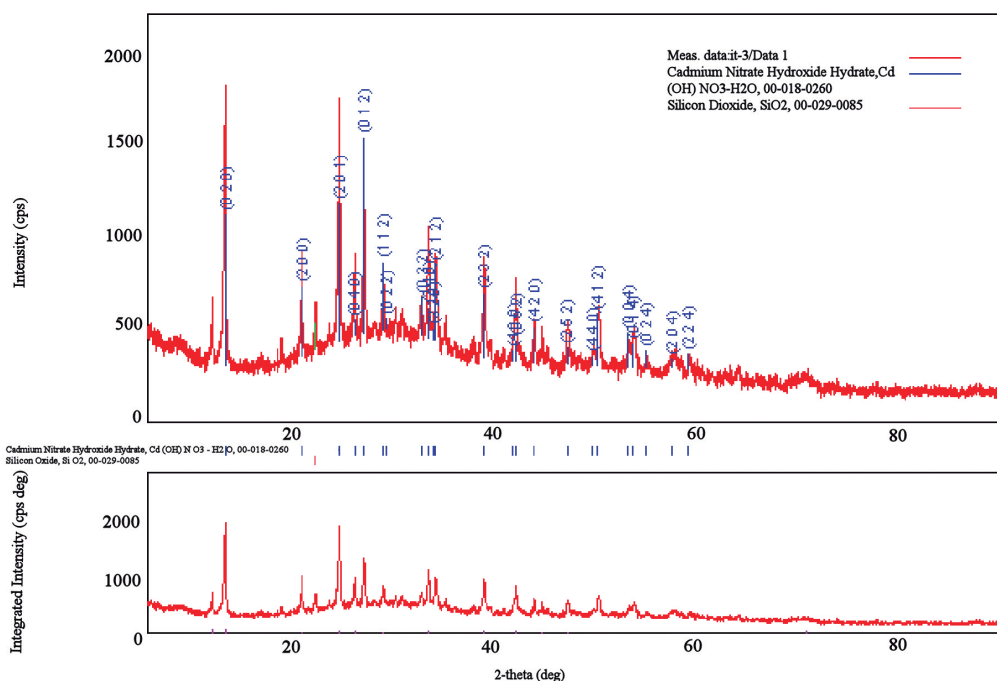


Fig 1. X-ray diffraction shows the Cd/SiNPs sample consisting of amorphous (the wide diffuse peak between 20 and 40 degrees) and crystalline phases. Database Searching confirms the presence of Cadmium Nitrate Hydroxide Hydrate, $\text{Cd}(\text{OH})\text{NO}_3 \cdot (\text{H}_2\text{O})$ (DB card number 00-018-0260), and silica (SiO_2 , DB card number 00-029-0085).

pollutants from possible impurities in the reagents or the grinding process in jars of tungsten carbide alloy with cobalt. The presence of Cd and Si has been highlighted (32.5% and 24.1% respectively), the main pollutants were Ca (0.3%), Na (0.2%), K (0.2%), Fe (0.04%) and Mn (0.001%). Other metals were present in quantities less than 1 %.

Characteristics of Cd/SiNPs

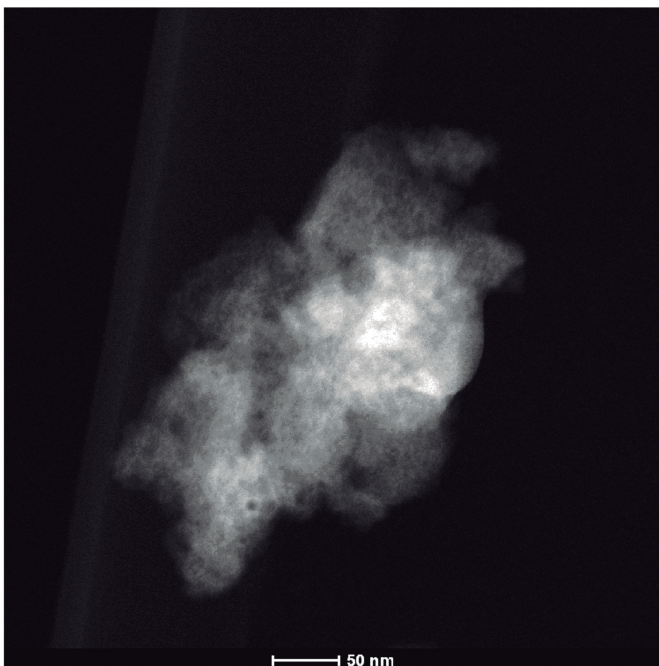
Table 1 summarizes major characteristics of the

Cd/SiNPs and SiNPs.

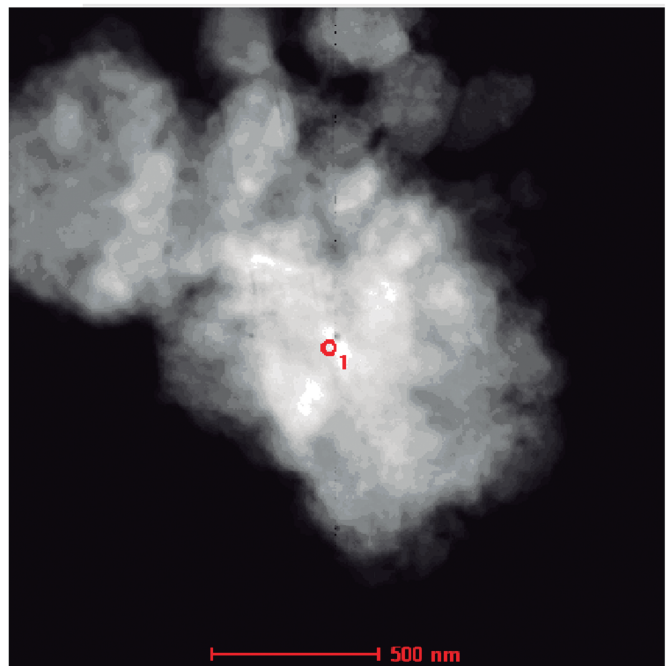
- X-ray diffraction showed that the sample seems to consists of amorphous (the wide diffuse peak between 20 and 40 degrees) and crystalline phases (Fig. 1). It was found that there is no one single phase in the database which provides a good match for all the peaks found for this sample. Database searching without any restrictions on a possible composition of the sample confirms the presence of Cadmium Nitrate Hydroxide Hydrate, $Cd(OH)NO_3 \cdot H_2O$ (DB card number 00-018-0260) and

STEM HAADF

a1



a2



b

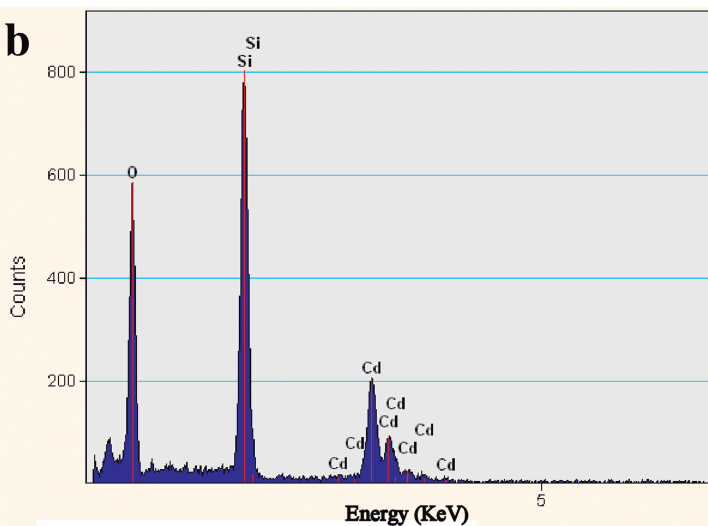


Fig. 2. STEM images of Cd/SiNPs. **a.** STEM analysis includes high-angle annular dark-field scanning transmission electron microscopy (HAADF STEM) images on the top (**a1** and **a2**). **b.** A energy dispersive X-ray spectrum (EDS) in the bottom. EDS analysis has been performed on the Cd/SiNPs indicated with an \circ in the insert and points out that the main composition of sample is Si, O, and Cd. In particular HAADF STEM images show the tendency to aggregate of Cd/SiNPs (that is, no isolated nanoparticles).

silica (SiO_2 , DB card number 00-029-0085).

- STEM quantitative analyses show the aggregation of Cd/SiNPs (Fig. 2A) and the analysis of the elements in HAADF mode (EDS spectra) confirmed the presence of Cd, Si and O in the Cd/SiNPs (Fig. 2B).

- Dynamic light scattering determination of the Cd/SiNPs and SiNPs size distribution shows a range of 50-500 nm for both types of nanoparticles (Fig. 3) and similar zeta potential between the two types of NPs (Table 1). Although particle samples were vortexed prior to measurement (similarly to what was performed before i.t. administration), a tendency to agglomerate was detected.

Animal body weight (b.w.)

The treated rats exposed to SiNPs or either form of Cd were not different from the controls in the rates of b.w. gain from day 0 (i.t. treatment) to the last day of treatment. During this period, the b.w. increased by 40% in all groups.

Lung histology

Cytohistological morphology

After i.t. exposure to all the different treatments, namely CdCl_2 , Cd/SiNPs and SiNPs, the lung parenchyma, analyzed by both light and electron microscopy, clearly showed patterns of injury with a different extent of intensity characterized by collapsed alveoli, areas with inflammatory alterations, granuloma

formation, thickening of alveolar septa and some patterns of bronchiolar epithelium exfoliation (Fig. 4). Noticeably, type II pneumocytes were clearly characterized by the presence of vacuolized and scarcely surfactant-lamellated bodies of various shapes and sizes. These morphological alterations were accompanied by expression changes of some molecules (e.g. different cytokines and metabolic factors, as reported below) typically involved in the tissue response reaction as a consequence of cytotoxic effects caused by the different instilled compounds. These overall effects were observed acutely (after 24 hr) and lasted until the 30th day, with Cd/SiNPs treatment producing the more marked effects compared to SiNPs and CdCl_2 groups.

Table 1. Physico-chemical characteristics of the silica nanoparticles.

	Cd/SiNPs	SiNPs
pH	7 *	7 *
Structure	both amorphous and crystalline	amorphous
Particle morphology	spherical form	spherical form
Primary particle size range	20-80 nm	60-90 nm
Specific Surface area BET	about 200 m^2/g	about 240 m^2/g
Tendency to aggregate and agglomerate	about 350 nm	about 120 nm
Zeta Potential	-23 mV *	-30 mV *

*: in deionized water.

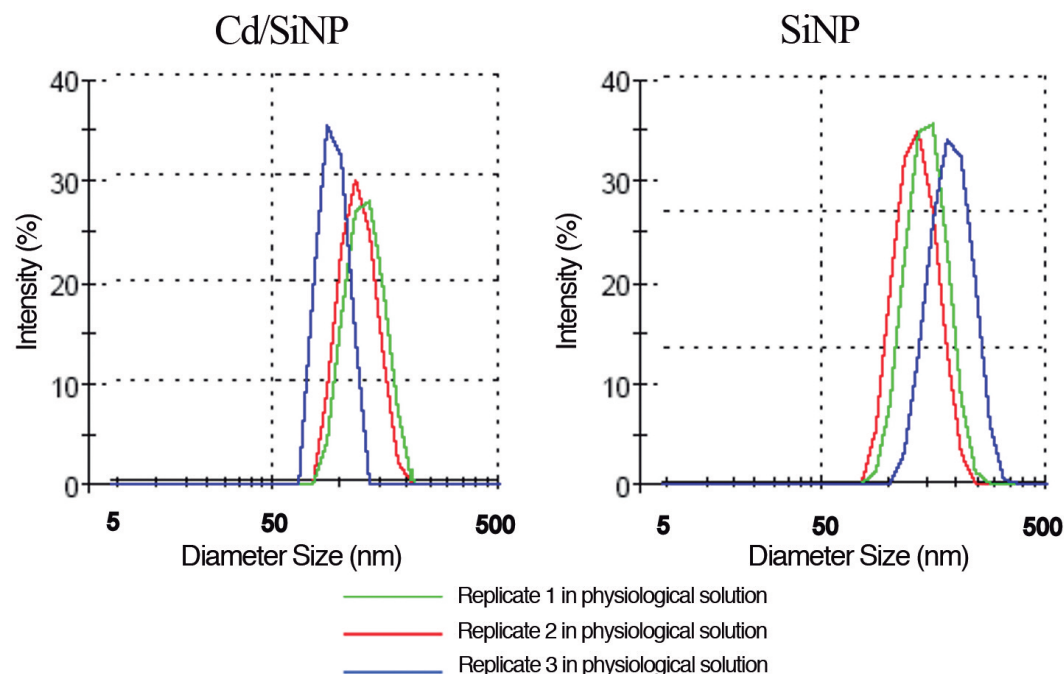


Fig. 3. Size distribution obtained from DLS measurements of Cd/SiNPs or SiNPs in physiological solutions.

Cell kinetics (cell death and proliferation) cytochemistry

To evaluate cell death as a consequence of CdCl_2 , SiNPs, Cd/SiNPs injury action in lungs, the cytochemical detection of DNA fragmentation with the TUNEL reaction was performed, while the lung cell proliferation response was determined by PCNA expression (Fig. 5A,B), as this accessory protein is mainly involved during the DNA replication and repair. Any presence of necrotic tissue was detected, while, on the contrary, several apoptotic cells were observed. The canonical apoptotic phenomenon, morphocytochemically characterized by nuclear pyknosis, karyorrhexis, TUNEL-positivity and apoptotic body formation (Fig. 6e-l) increased significantly after all three types of treatment more markedly at the early time

point (24 hr) and persisting for 30 days (with tendency to decrease with time) (Fig. 5). However, this enhancement was more pronounced for Cd/SiNPs> CdCl_2 >SiNPs. The more marked effects caused by Cd/SiNPs were mainly in the alveolar epithelial cells in comparison to the bronchiolar epithelial cells and the macrophages.

With regard to PCNA expression, a significant increased number of immunoreactive proliferating pulmonary cells was detected, both at epithelial and stromal levels (Fig. 6a-b) for all types of treatment, and in parallel, at ultrastructural level, high mitotic activity was also seen (Fig. 6c-d): SiNPs and CdCl_2 produced a similar increase for all time points considered, while the effect of Cd/SiNPs was more pronounced at 1 and 7 day-post treatment with a mild attenuation at the 30th day (Fig. 5B).

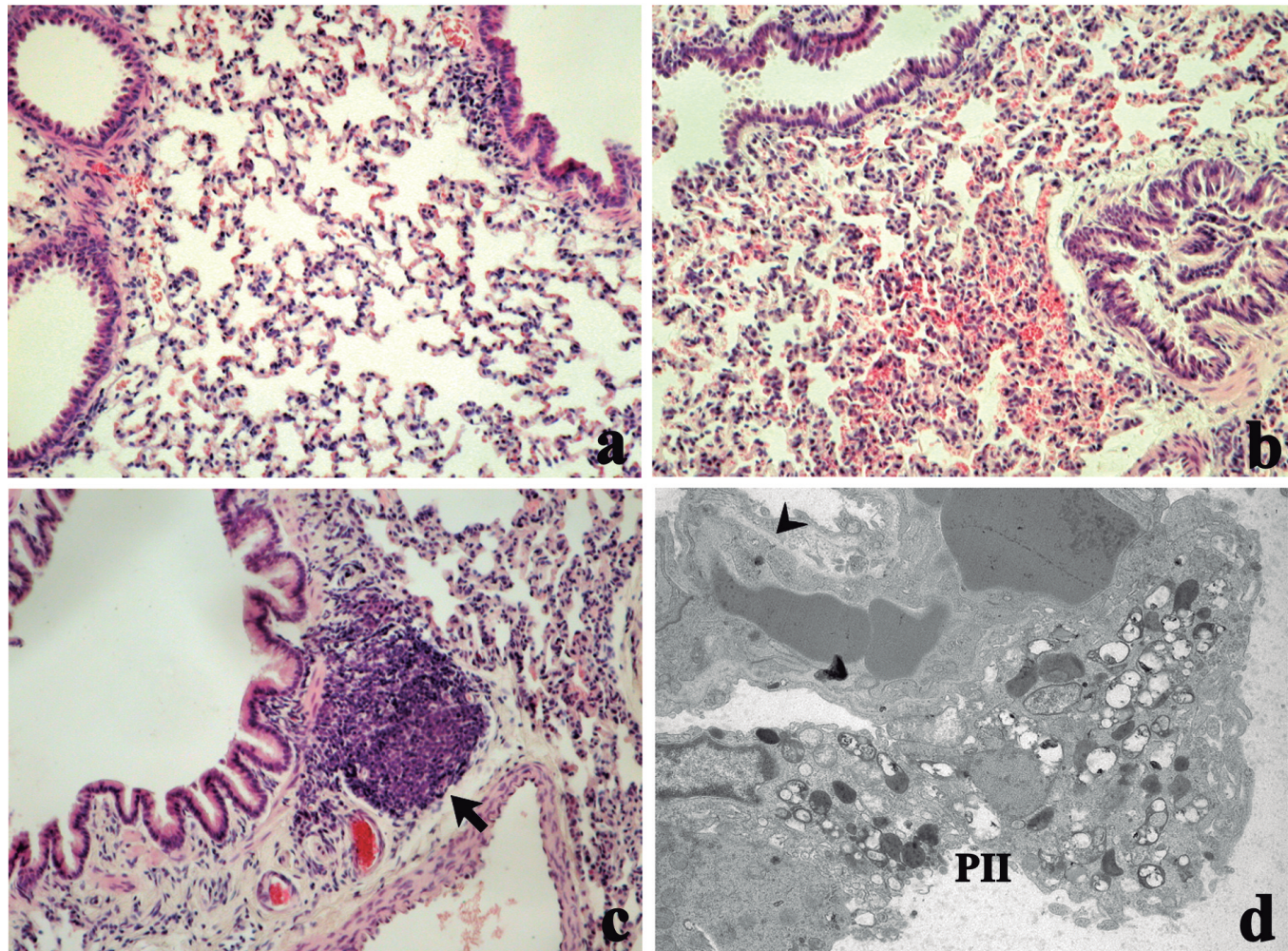


Fig. 4. Light microscopy (H&E: a-c) and electron microscopy (d) of some structural changes detected in lung parenchyma of control (a) and Cd/SiNPs-treated animals (b-d). **a.** Normal alveolar and bronchiolar morphology. **b.** Collapsed alveoli with wall thickening and micro-hemorrhagic foci, associated with bronchiolar distortion and epithelial cell desquamation. **c.** Bronchus-associated prominent lymphoid nodule (arrow) in the peribronchiolar and perivascular areas. **d.** Ultrastructure of edematous alveolar wall (arrow) and type II pneumocytes (PII) filled by vacuolated multi-vesicular bodies. a-c, x 40; d, x 4,400

Cytokine and chemokine immunocytochemistry

The cellular localization and distribution of IL-6, IP-10, and TGF- β 1, all involved in tissue injury and repair pathways, revealed an extensive spreading in the bronchiolar, alveolar and stromal cells, evidencing the cellular inflammatory response, which was more intense for Cd/SiNPs already observable at 24 hr and which persisted at 30 days (Table 2).

The heaviest IL-6-immunopositivity after Cd/SiNPs was detected at the stromal level, with several immunopositive fibroblasts and endothelial cells staining in alveolar areas. Similar staining was seen after CdCl_2 , as well as after SiNPs (Fig. 7a-e).

A marked IP-10-immunoreactivity was detected at the alveolar wall (endothelium and macrophages) and

bronchiolar levels (airway epithelium), particularly after Cd/SiNPs and CdCl_2 (Fig. 7f-l).

The TGF- β 1 antigen appeared significantly more expressed in the stromal cells (e.g. macrophages and fibroblasts) and in the collapsed alveolar areas (Fig. 7 m-q) during macrophage activation and fibrosis induction. Eotaxin-1, a CC chemokine involved in eosinophil recruitment and activation causing inflammatory damage to the airway in particular allergic disease (i.e. asthma), was not modified by any treatment (data not shown).

Metabolic factor and collagen immunocytochemistry

CYP450-immunoreactivity was significantly enhanced, in a time-dependent manner (24 hr < 7 days < 30 days), and this was particularly evident at bronchiolar (e.g. Clara cells) and alveolar (e.g. macrophages) level (Fig. 8 a-c) after both Cd/SiNPs and CdCl_2 . SiNPs did not influence CYP450 epitope immunolabeling (Table 2). Noticeably, numerous CYP450-immunopositive activated Clara cells were detected in the bronchiolar epithelium of treated animals, which appeared heavily basophilic and showed apical protrusion containing several electron-dense secretary granules (Fig. 8d-e).

None of the treatments altered the calcium-binding protein, Calmodulin-like immunoreactivity (data not shown).

Immunocytochemistry for Type I collagen showed that at 7 and 30 days after Cd/SiNPs exposure a strong fibrogenic reaction occurred (Table 2). As collagen (Type I) concerns, the immunocytochemical labelling

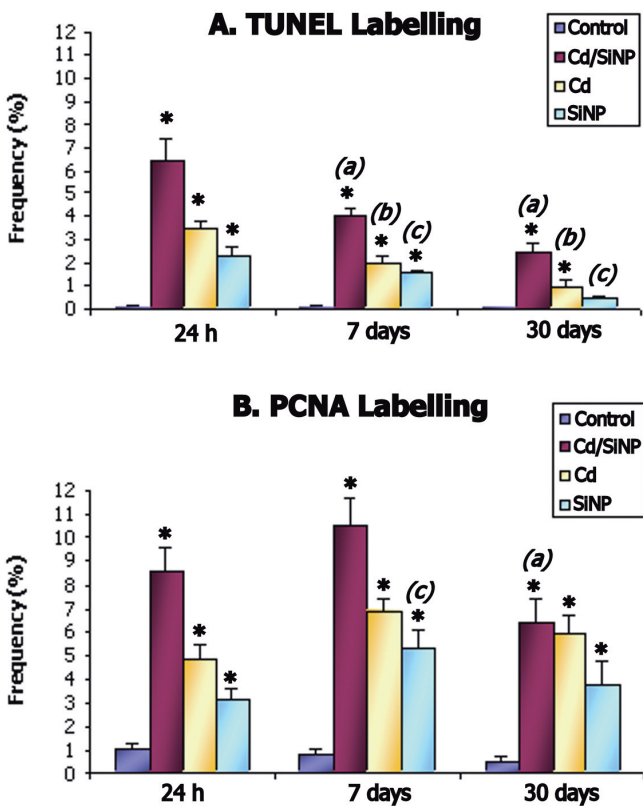


Fig. 5. Histograms showing changes in percentage of TUNEL (A) and PCNA (B) Labelling Index of pulmonary cells as a consequence of i.t. exposure to different substances: CdCl_2 (Cd) versus Silica nanoparticles bare (SiNP) or Cadmium-doped (Cd/SiNP) measured at three different time points (24 hr, 7 and 30 days). In all treated rats, a significant increase (two-way ANOVA) of positive cells was clearly observed, more markedly at the early time point (24 hr), lasting until 30 days (with tendency to decrease with time) showing the trend Cd/SiNPs> CdCl_2 >SiNPs. Data are expressed as mean \pm S.D. (*) signifies statistically significant differences ($p < 0.05$) compared to the respective control. Different letters (a-c) denote mean values that are statistically different at $p < 0.05$: comparison is between one time point versus the one immediately before of the same group.

Table 2. Expression of immunolabelling for IL-6, TGF- β 1, IP-10, CYP 450 and Collagen (Type I) on a semiquantitative evaluation.

	Control	24 hr	7 days	30 days	p Value
Cd/SiNPs					
IL-6	\pm	++++	+++	++ \pm	**
TGF- β 1	\pm	+++	++++	++	**
IP-10	\pm	++++	++++	++ \pm	**
CYP 450	\pm	++	++ \pm	+++	**
Collagen-I	\pm	\pm \pm	+++	++ \pm	**
CdCl_2					
IL-6	\pm	+++	++ \pm	++	**
TGF- β 1	\pm	++	+++	++ \pm	**
IP-10	\pm	+++	++ \pm	++	**
CYP 450	\pm	+	++	++ \pm	*
Collagen-I	\pm	\pm \pm	+++	++	*
SiNPs					
IL-6	\pm	+++	++	++ \pm	*
TGF- β 1	\pm	++	++ \pm	+	*
IP-10	\pm	+++	++ \pm	++	*
CYP 450	\pm	+	++	++	NS
Collagen-I	\pm	\pm \pm	+++	++	*

Degree of staining intensity: from undetectable (-) to strong (++++). p values calculated by Kruskal-Wallis test: (**) < 0.01 ; (*) < 0.05 .

changes between control and treated rats, also supported by TEM analyses, appeared evident particularly 7 and 30 days after Cd/SiNPs exposure (Table 2), when a strong

stromal fibrogenic reaction occurred, characterized by diffuse collagen fiber deposition both in juxta-bronchiolar areas and within the alveolar walls (Fig. 9a-f).

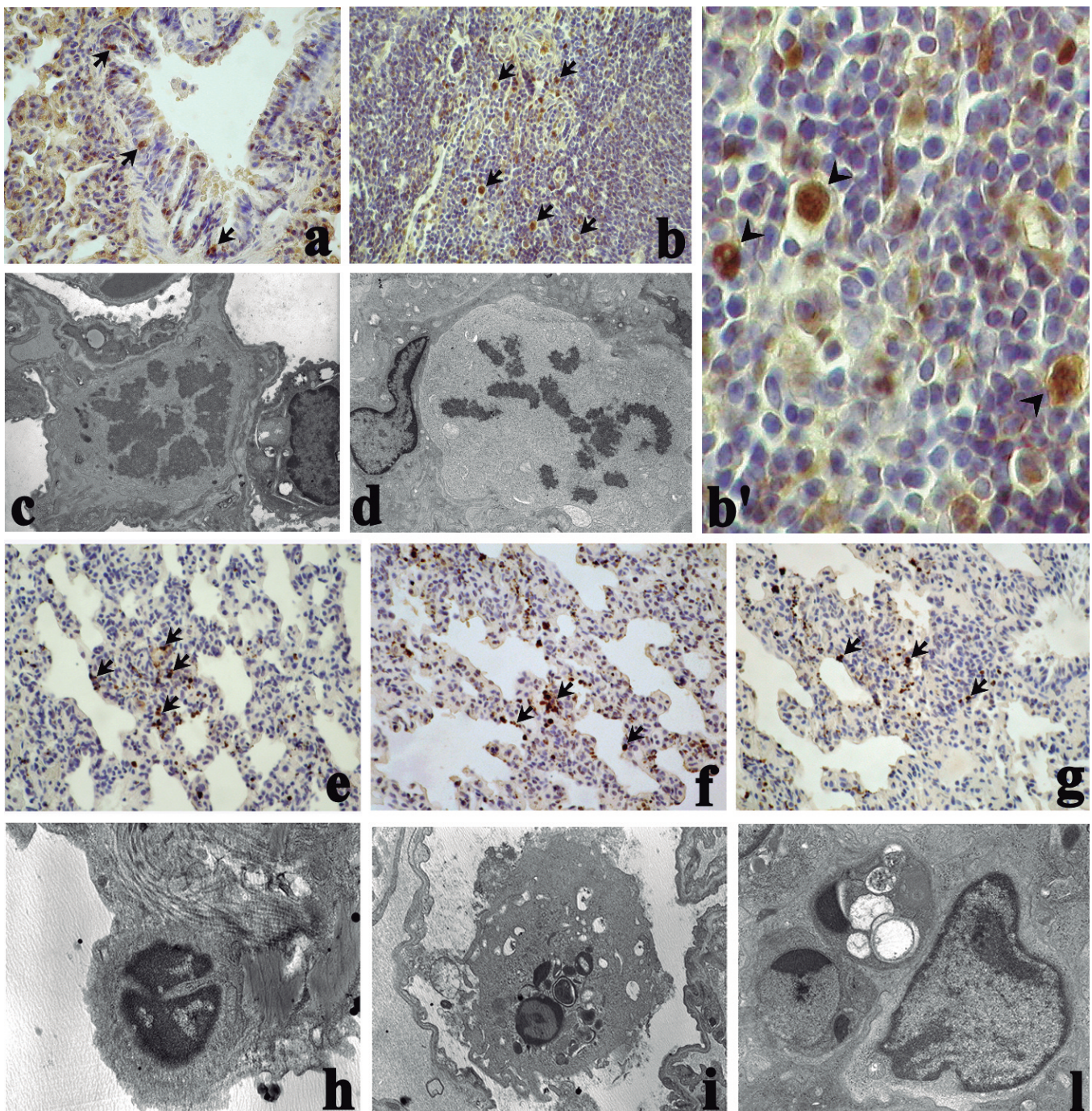


Fig. 6. Cell proliferation (a-b') and apoptosis (e-g) detected by PCNA immunolabelling and TUNEL staining respectively, detected 24 hr (e, g) and 30 days (a-b' and f) after rat i.t. exposure to 1 mg/kg b.w. Cd/SiNPs (a-b and e-f) and CdCl_2 (a-b and f-g). PCNA positive epithelial cells (arrows) at bronchiolar (a) and stromal levels (b-b'); particularly, in (b-b') a juxta-nodular collapsed area is presented, showing active proliferating inflammatory cell infiltration (arrowheads); TUNEL positive cells (chromatin condensation) detected in stromal and epithelial areas (e-g), in which labelled pneumocytes and macrophages (arrows) were observable. Electron micrographs showing alveolar and stromal mitoses (c-d) and different phases of apoptotic cell death: pyknosis (h), karyorhexis (i) and apoptotic body formation (l). a, b, e-g, $\times 40$; b', $\times 100$; c, $\times 4,400$; d, $\times 3,000$; h, $\times 12,000$; i, l, $\times 7,000$

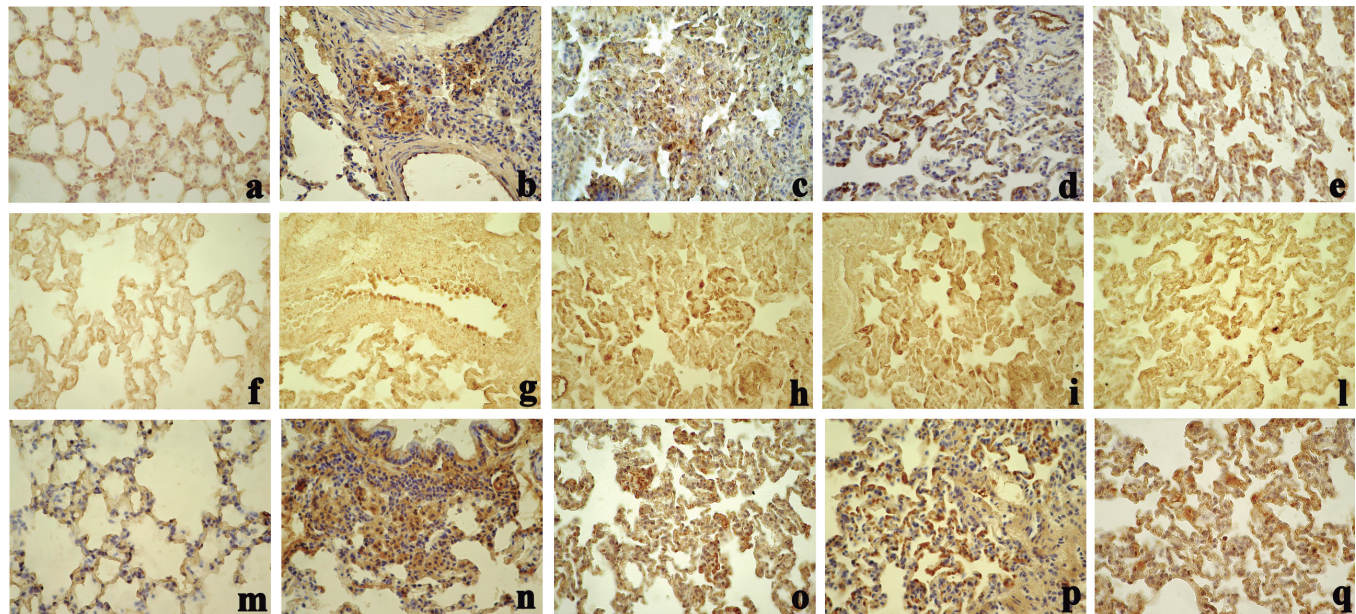


Fig. 7. Immunostaining patterns of IL-6 (a-e), IP-10 (f-l) and TGF- β 1 (m-q) expression in controls (a, f, and m) and rats differently treated with Cd/SiNPs (b-c, g-h and n-o) or CdCl₂ (d, i, p) or SiNPs (e, l, q), at 24 hr (b-e, g-l) or 7 days (n-q) after i.t. exposure. Noticeably, low labelling for IL-6 is detected at all lung districts (e.g. bronchiolar, stromal and alveolar levels) in controls (a), while, 24 hr after all treatments, bronchiolar, stromal and, sometimes collapsed, alveolar areas appeared strongly immunoreactive for IL-6 (b-e) and IP-10 (g-l), showing several marked immunopositive cells (arrows). Strong immunoreactivity for TGF- β 1 is observed mainly at stromal level (n) and in several collapsed alveolar zones (o-q) with evident immunopositivity at endothelial level. x 40.

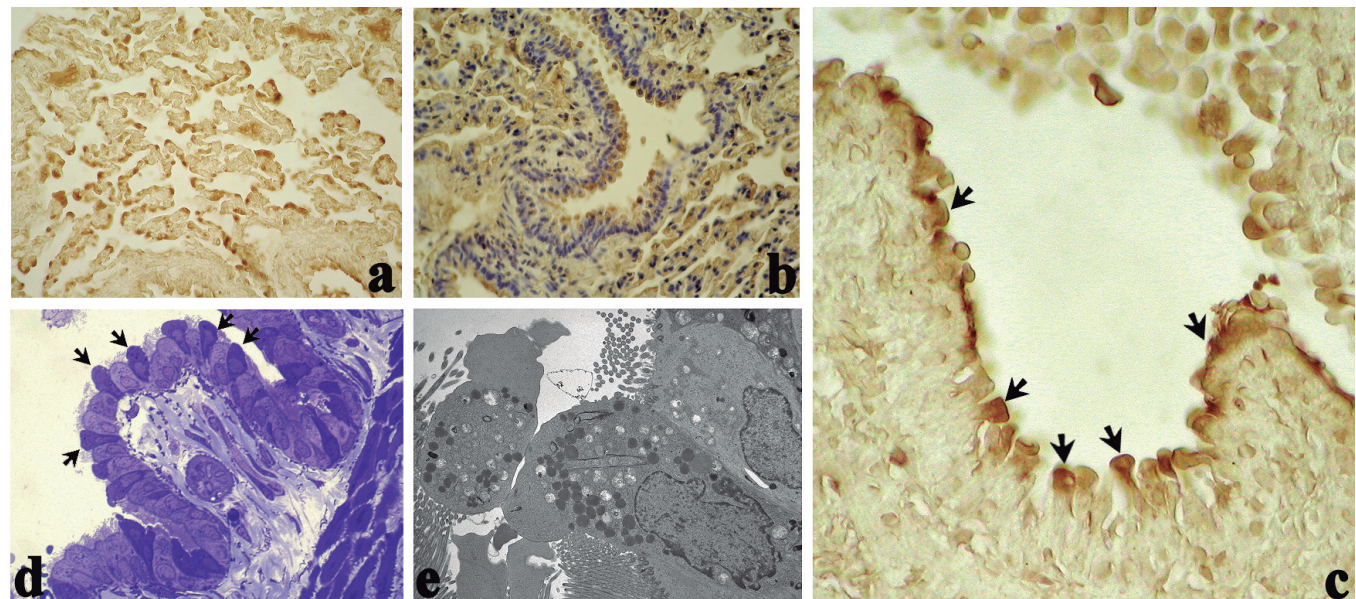


Fig. 8. Immunostaining reaction for CYP450 (a-c) in lung 30 days after i.t exposure to Cd/SiNPs. Significantly enhanced CYP450-immunoreactivity, evident at alveolar (a) and bronchiolar levels (b) was detected; particularly, the presence of several activated CYP450-immunopositive Clara cells (arrows) was detected in the apical region of bronchiolar epithelium (c). Light (methylene blue staining on semithin sections), (d) and electron microscopy (e) details similarly demonstrating the occurrence of numerous activated Clara cells (arrows). a, b, x 40; c, x 60; d, x 100; e, x 3,000

Discussion

The present study has addressed the pulmonary effects of new ENPs “Cd/SiNPs” versus SiNPs and CdCl_2 on some cell kinetic and cytochemical parameters investigated in rats at different time points post treatment (single i.t. exposure to 1 mg/rat, 600 $\mu\text{g}/\text{rat}$ and 400 $\mu\text{g}/\text{rat}$, respectively).

The findings clearly demonstrate that Cd/SiNPs other than SiNPs and CdCl_2 produce a general pulmonary toxicity coupled with an inflammatory response, noticeably deductible by the occurrence of a widespread cellular reaction aimed to obstacle and recover tissue damage, observed both at epithelial and stromal levels, with signs of fibrosis and granulomas formation. The effects were detectable at the earliest time point, 24 h, and persisted until the 30th day, and more markedly for Cd/SiNPs group.

Our experimental results, showing inflammation and fibrosis, evidenced by a wide-spread immunoreactivity of both cytokines/chemokines and collagen, respectively, are in agreement with previous literature data for either CdCl_2 or SiNPs reporting toxic pulmonary effects. In fact, several experimental studies using similar treatment protocol reported that CdCl_2 induces lung histopathological alterations (i.e., inflammation and fibrosis) at 7 days after treatment, still present 90 days post-exposure with a greater extent of lesions compared to

those observed at 28 days (Damiano et al., 1990; Driscoll et al., 1992; Bell et al., 1997). Ultrafine silica (amorphous or colloidal) particles (1-3 mg/mouse), administrated by i.t., produced acute and chronic granulomatous inflammation (at the later stage - 14 weeks) (Cho et al., 2007), as well as acute bronchiolar degeneration, necrosis, neutrophilic infiltration, alveolar type II cell swelling and alveolar macrophage accumulation (Kaewamatawong et al., 2005). However, lower instillation doses (0.3-30 $\mu\text{g}/\text{lung}$) of ultrafine colloidal silica particles demonstrated a transient acute moderate lung inflammation and tissue damage, associated with oxidative stress and apoptosis, since these inflammatory responses receded and recovered after 30 days (Kaewamatawong et al., 2006). The same authors suggested that concentration of less than 0.3 $\mu\text{g}/\text{lung}$ was not associated with toxic pulmonary effects in mice. Moreover, the effect of nano- SiO_2 (20 mg silica dust, i.t.) on fibrogenesis was demonstrated during a 2-month-study in rats with, however, a milder effect than that of micron- SiO_2 suggesting that SiO_2 , nanoparticles, because of their size, probably diffuse more easily to extrapulmonary compartments than microparticles (Chen et al., 2004).

From a cytokinetic point of view, our findings demonstrate a correlation between cell loss, (namely epithelial cell exfoliation and apoptosis) and cell proliferation, which may represent the primary reaction

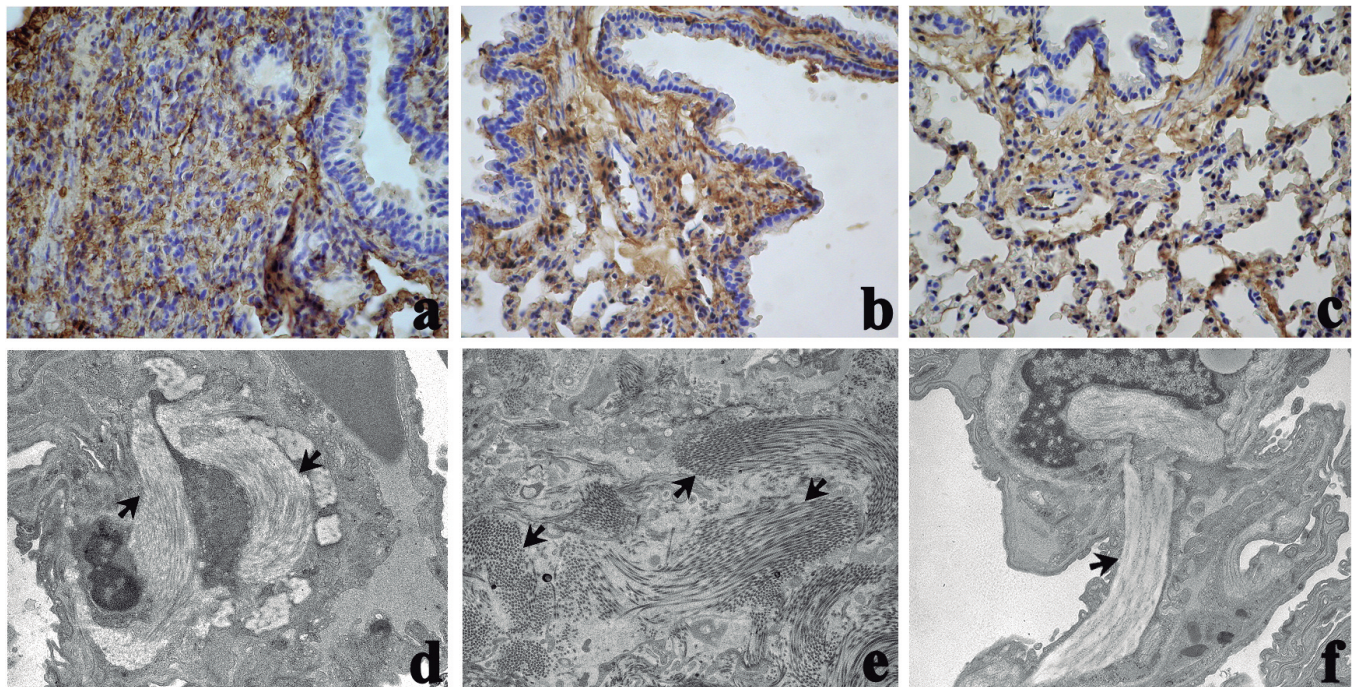


Fig. 9. Immunostaining reaction for Collagene Type I (a-c) in lung, 7 and 30 days (a, c and b, respectively) after i.t exposure to Cd/SiNPs (a-b) or SiNPs (c). The collagen-labelling changes between control and treated rats appeared evident, particularly 7 and 30 days after Cd/SiNPs (a and b, respectively) and 30 days after SiNPs (c) exposure, with a strong stromal fibrogenic reaction characterized by diffuse collagen storage (a-c). TEM images (d-f) similarly showed enhanced collagen fiber deposition (arrows) in the alveolar and stromal areas. a-c, $\times 40$; d, f, $\times 7,000$; e, $\times 4,400$

of both epithelial and stromal cells against the acute insult by all instilled compounds. The apoptosis lasted until the 30th day post instillation with a tendency to decrease over time. This phenomena is accompanied by an increase of proliferating pulmonary cells, as shown by the occurrence of several mitoses both at epithelial and stromal levels, clearly indicating the cellular response aimed at structural remodelling of damaged alveoli. The presence of cell populations undergoing apoptosis and epithelial desquamation, more frequent after Cd/SiNPs exposure, suggest an injury condition mainly involving the airway and alveolar lining cells. Recent findings of nanosilica in pulmonary cells undergoing apoptosis have suggested that apoptosis is one of the mechanisms of silica-related cell damage in humans (Song et al., 2011).

In addition, our study indicates that, other than cell proliferation and repair as mechanisms compensating cell loss, tissue recovery is also accompanied by an interstitial reaction represented by a gradual increase production of extracellular matrix in a time-dependent manner. Specifically, our results underline the pivotal role of interstitial type I collagen overexpression in creating abnormal spatial organization of the alveolar septa at different temporal stages, being, type I, the major collagen present in extracellular matrix and perhaps the most important factor for stabilization of tissue structure, growth and repair. In line with literature data, this fibrotic response that we observed in a delayed manner (starting to be manifest at 7 days post i.t.) is typical of the presently tested materials (i.d. SiNPs and CdCl₂). Differently, our previous studies demonstrated that i.t. exposure to multiwalled carbon nanotubes produced a general pulmonary toxicity coupled with inflammatory response without overt signs of fibrosis and granuloma formation, even at 16 days after their instillation in rats (Roda et al., 2011).

Regarding the chemokines, our data, showing an early occurrence followed by a persistence of increased cytokines-immunoreactivity (i.e., IL-6, TGF- β 1, and IP-10), are in agreement with the notion that an active pulmonary remodelling after injury is typically characterized by an increase of cytokine mediator levels (Branton and Kopp, 1999; Yu et al., 2002; Choi et al., 2008). In particular, TGF- β 1 may function as a master switch in tissue repair and wound healing, even though substantial evidence indicated that a continuous disordered expression of TGF- β 1 may lead to fibrosis (Willis et al., 2005). Moreover, pulmonary fibroblast proliferation would be an indirect effect of TGF- β 1 increase which in turn may induce fibroblasts to differentiate into myofibroblasts, the latter representing the main source of extracellular matrix material during lung fibrogenesis (Agostini and Gurrieri, 2006). The pro-inflammatory cytokines, such as IL-6, TGF- β 1, and IP-10, are essential in the progression of pulmonary diseases, for example from early pulmonary inflammation to the outcome of fibrosis, being important mediators for recruiting various cell types including

alveolar epithelial and endothelial cells, alveolar macrophages, fibroblasts and activated lymphocytes (Agostini et al., 2000; Shiozawa et al., 2004; Kim et al., 2009). A recent study demonstrated overexpression of the chemokine receptor CXCR3 and its ligands (including IP-10) in chronic obstructive pulmonary disease (Kelsen et al., 2009). On the other hand, IL-6 has been reported to have both pro-inflammatory and anti-inflammatory capabilities. Regarding the latter effects, several studies showed IL-6 ability to inhibit the production of tumor necrosis factor, IL-1 β and macrophage inflammatory protein-2, to stimulate the production of metalloproteinase inhibitors, to reduce intracellular superoxide production, and to inhibit cellular apoptosis (Yu et al., 2002).

Concerning the morphological alterations, in the present study the occurrence of alveolar type II pneumocytes containing multivesicular bodies with scarce lamellar structures indicates a decrease of surfactant secretion to the extracellular milieu as a consequence of cell damage. The relevance of this surfactant alteration comes from the fact that this product plays a crucial role in the prevention of alveolar collapse by reducing surface tension, interstitial oedema and hyaline membranes (Alarifi et al., 2004).

Moreover, our findings indicate for the first time that both CdCl₂ and Cd/SiNPs are able to modulate the CYP450 in lung tissue (e.g. in Clara cells and alveolar macrophages) at all time points considered. Several studies indicate that alveolar macrophages play an important role as defence cells against inhaled particles by expression of cyp genes (e.g. cytochrome P450) in addition to Clara cells of the bronchiolar epithelium (Voit Fanucchi et al., 1997; Hukkanen et al., 2001; Saarikoski et al., 2005). Scarce literature data report cadmium effects on hepatic cytochrome P450 (CYP450) content after *in vivo* administration (Pillai and Gupta, 2005) and nanoparticles (Carboxyl polystyrene latex beads) effects on CYP450 system in *in vitro* hepatic models (Fröhlich et al., 2010).

In conclusion, although the use and application in nanotechnology of SiNPs is promising, the risk associated with new nanomaterials needs to be assessed. The present findings suggest that ENPs such as Cd/SiNPs are toxic to lung tissue after i.t. exposure, even more than SiNPs alone and the pneumotoxicant CdCl₂.

For the present study i.t. was applied as a useful method to compare lung effects in rats of a new material (i.e., counterpart-doped nanoparticles) against similar compounds (i.e. CdCl₂) for which an extensive inhalation database is available (ATSDR, 2008). Moreover, the i.t. model may serve as a screening tool to determine the approximate dose range that may be appropriate for later inhalation studies, mimicking realistic conditions of human respiratory exposure as may occur in environmental and occupational setting, as well as to address specific endpoints regarding the respiratory toxicity of nanomaterials (Driscoll et al., 2000).

Acknowledgements. We would like to thank Dr. Sujing Xie, Dr. Kurt Langworthy, Dr. Lev Zakharov, and Dr Chris Larson from CAMCOR, University of Oregon (Eugene, OR, USA) for their valuable support and assistance in the physico-chemical characterization of Cd/SiNPs. The authors wish to acknowledge Mr. Davide Acerbi for his excellent technical assistance and Ms. Gloria Milanesi for the preparation of the electron microscopy specimens.

Declaration of interest. This work was supported by the Italian Ministries of Health, Research and Education (PRIN 2007) and by Cariplò 2009 grant. The authors report no declaration of interests. The Authors alone are responsible for the content and writing of the paper.

References

- ATSDR (Agency for Toxic Substances and Disease Registry) (2008). Toxicological profile for Cadmium (Draft for Public Comment). Atlanta, GA: U.S. Department of Health and Human Services, Public Health Service.
- Agostini C. and Gurrieri C. (2006). Chemokine/cytokine cocktail in idiopathic pulmonary fibrosis. *Proc. Am. Thorac. Soc.* 3, 357-363.
- Agostini C., Facco M., Siviero M., Carollo D., Galvan S., Cattelan A.M., Zambello R., Trentin L. and Semenzato G. (2000). CXC chemokines IP-10 and mig expression and direct migration of pulmonary CD8+/CXCR3+ T cells in the lungs of patients with HIV infection and T-cell alveolitis. *Am. J. Respir. Crit. Care Med.* 162, 1466-1473.
- Alarifi S.A., Mubarak M.M. and Alokail M.S. (2004). Ultrastructural changes of pneumocytes of rat exposed to Arabian incense (Bakhour). *Saudi Med. J.* 25, 1689-1693.
- Barik T.K., Sahu B. and Swain V. (2008). Nanosilica-from medicine to pest control. *Parasitol. Res.* 103, 253-258.
- Bell R.R., Soliman M.M., Nonavinkere V.K., Hammerbeck D.M. and Early J.L. 2nd (1997). Selenium and cadmium induced pulmonary functional impairment and cytotoxicity. *Toxicol. Lett.* 90, 107-114.
- Bell R.R., Nonavinkere V.K. and Soliman M.R. (2000). Intratracheal exposure of the guinea pig lung to cadmium and/or selenium: a histological evaluation. *Toxicol. Lett.* 114, 101-109.
- Bharali D.J., Klejbor I., Stachowiak E.K., Dutta P., Roy I., Kaur N., Bergey E.J., Prasad P.N., Stachowiak M.K. (2005). Organically modified silica nanoparticles: a nonviral vector for *in vivo* gene delivery and expression in the brain. *Proc. Natl. Acad. Sci. USA* 102, 11539-11544.
- Branton M.H. and Kopp J.B. (1999). TGF-beta and fibrosis. *Microbes Infect.* 1, 1349-1365.
- Chen Y., Chen J., Dong J. and Jin Y. (2004). Comparing study of the effect of nanosized silicon dioxide and microsized silicon dioxide on fibrogenesis in rats. *Toxicol. Ind. Health* 20, 21-27.
- Cho W.S., Choi M., Han B.S., Cho M., Oh J., Park K., Kim S.J., Kim S.H. and Jeong J. (2007). Inflammatory mediators induced by intratracheal instillation of ultrafine amorphous silica particles. *Toxicol. Lett.* 175, 24-33.
- Choi M., Cho W.S., Han B.S., Cho M., Kim S.Y., Yi J.Y., Ahn B., Kim S.H. and Jeong J. (2008). Transient pulmonary fibrogenic effect induced by intratracheal instillation of ultrafine amorphous silica in A/J mice. *Toxicol. Lett.* 182, 97-101.
- Damiano V.V., Cherian P.V., Frankel F.R., Steeger J.R., Sohn M., Oppenheim D. and Weinbaum G. (1990). Intraluminal fibrosis induced unilaterally by lobar instillation of CdCl₂ into the rat lung. *Am. J. Pathol.* 137, 883-894.
- De Jong W.H. and Borm P.J. (2008). Drug delivery and nanoparticles: applications and hazards. *Int. J. Nanomedicine* 3, 133-149.
- Donaldson K., Stone V., Cluster A., Renwick L. and MacNee W. (2001). Ultrafine particles. *Occup. Environ. Med.* 58, 211-216.
- Driscoll K.E., Maurer J.K., Poynter J., Higgins J., Asquith T. and Miller N.S. (1992). Stimulation of rat alveolar macrophage fibronectin release in a cadmium chloride model of lung injury and fibrosis. *Toxicol. Appl. Pharmacol.* 116, 30-37.
- Driscoll K.E., Costa D.L., Hatch G., Henderson R., Oberdörster G., Salem H. and Schlesinger R.B. (2000). Intratracheal instillation as an exposure technique for the evaluation of respiratory tract toxicity: uses and limitations. *Toxicol. Sci.* 55, 24-35.
- Fröhlich E., Kueznik T., Samberger C., Roblegg E., Wrighton C. and Pieber T.R. (2010). Size-dependent effects of nanoparticles on the activity of cytochrome P450 isoenzymes. *Toxicol. Appl. Pharmacol.* 242, 326-332.
- Fubini B. and Hubbard A. (2003). Reactive oxygen species (ROS) and reactive nitrogen species (RNS) generation by silica in inflammation and fibrosis. *Free Radic. Biol. Med.* 34, 1507-1516.
- Gemeinhart R.A., Luo D. and Saltzman W.M. (2005). Cellular fate of a modular DNA delivery system mediated by silica nanoparticles. *Biotechnol. Progr.* 21, 532-537.
- Hukkanen J., Pelkonen O. and Raunio H. (2001). Expression of xenobiotic-metabolizing enzymes in human pulmonary tissue: possible role in susceptibility for ILD. *Eur. Respir. J.* 18 (suppl 32), 22s-126s.
- IARC (International Agency for Research on Cancer) (1993). Cadmium and cadmium compounds. IARC Monogr. Eval. Carcinog. Risk Hum. 58, 119-237.
- IARC (International Agency for Research on Cancer) (1997). Working Group on the Evaluation of Carcinogenic Risks to Humans. Silica, some silicates, coal dust and para-aramid fibrils. 68, 1-475.
- Joseph P. (2009). Mechanisms of cadmium carcinogenesis. *Toxicol. Appl. Pharmacol.* 238, 272-279.
- Kaewamatawong T., Kawamura N., Okajima M., Sawada M., Morita T. and Shimada A. (2005). Acute pulmonary toxicity caused by exposure to colloidal silica: particle size dependent pathological changes in mice. *Toxicol. Pathol.* 33, 743-749.
- Kaewamatawong T., Shimada A., Okajima M., Inoue H., Morita T., Inoue K. and Takano H. (2006). Acute and subacute pulmonary toxicity of low dose of ultrafine colloidal silica particles in mice after intratracheal instillation. *Toxicol. Pathol.* 34, 958-965.
- Kelsen S.G., Aksoy M.O., Georgy M., Hershman R., Ji R., Li X., Hurford M., Solomides C., Chatila W. and Kim V. (2009). Lymphoid follicle cells in chronic obstructive pulmonary disease overexpress the chemokine receptor CXCR3. *Am. J. Respir. Crit. Care Med.* 179, 799-805.
- Kim J.Y., Choeng H.C., Ahn C. and Cho S-H. (2009). Early and late changes of MMP-2 and MMP-9 in Bleomycin-induced pulmonary fibrosis. *Yonsei Med. J.* 50, 68-77.
- Lee K.P. and Kelly D.P. (1992). The pulmonary response and clearance of Ludox colloidal silica after a 4-week inhalation exposure in rats. *Fundam. Appl. Toxicol.* 19, 399-410.
- Li X.Y., Brown D., Smith S., MacNee W. and Donaldson K. (1999). Short-term inflammatory responses following intratracheal instillation of fine and ultrafine carbon black in rats. *Inhal. Toxicol.* 11, 709-731.
- Maynard A.D., Aitken R.J., Butz T., Colvin V., Donaldson K.,

- Oberdörster G., Philbert M.A., Ryan J., Seaton A., Stone V., Tinkle S.S., Tran L., Walker N.J. and Warheit D.B. (2006). Safe handling of nanotechnology. *Nature* 444, 267-269.
- Napierska D., Thomassen L.C.J., Lison D., Martens J.A. and Hoet P.H. (2010). The nanosilica hazard: another variable entity. Part Fibre Toxicol. 7, 39, [http://www.particleandfibretoxicology.com/content/7/1/39](http://www.particleandfibretotoxicology.com/content/7/1/39).
- Nemmar A., Hoylaerts M.F., Hoet P.H., Vermylen J. and Nemery B. (2003). Size effect of intratracheally instilled particles on pulmonary inflammation and vascular thrombosis. *Toxicol. Appl. Pharmacol.* 186, 38-45.
- Oberdörster G. (1992). Pulmonary deposition, clearance and effects of inhaled soluble and insoluble cadmium compounds. In: Cadmium in the human environment: Toxicity and carcinogenicity. Nordberg G.F., Herber R.F.M. and Alessio L. (eds). International Agency for Research on Cancer. Lyon. pp 189-204.
- Oberdörster G., Cherian M.G. and Baggs R.B. (1994). Correlation between cadmium-induced pulmonary carcinogenicity, metallothionein expression, and inflammatory processes: a species comparison. *Environ. Health Perspect.* 102 (suppl 3), 257-263.
- Oberdörster G., Oberdörster E. and Oberdörster J. (2005). Nanotoxicology: an emerging discipline evolving from studies of ultrafine particles. *Environ. Health Perspect.* 113, 823-839.
- Park E-J., Roh J., Kim Y. and Choi K. (2011). A single instillation of amorphous silica nanoparticles induced inflammation responses and tissue damage until day 28 after exposure. *J. Health Sci.* 57, 60-71.
- Pillai A. and Gupta S. (2005). Effect of gestational and lactational exposure to lead and/or cadmium on reproductive performance and hepatic oestradiol metabolising enzymes. *Toxicol. Lett.* 155, 179-186.
- Potts R.J., Bespalov I.A., Wallace S.S., Melamede R.J. and Hart B.A. (2001). Inhibition of oxidative DNA repair in cadmium-adapted alveolar epithelial cells and the potential involvement of metallothionein. *Toxicology* 161, 25-38.
- Ravi Kumar M.N.V., Sameti M., Mohapatra S.S., Kong X., Lockey R.F., Bakowsky U., Lindenblatt G., Schmidt C.H. and Lehr M. (2004). Cationic silica nanoparticles as gene carriers: synthesis, characterization and transfection efficiency *in vitro* and *in vivo*. *J. Nanosci. Nanotechnol.* 4, 876-881.
- Reuzel P.G., Bruijntjes J.P., Feron V.J. and Woutersen R.A. (1991). Subchronic inhalation toxicity of amorphous silicas and quartz dust in rats. *Food Chem. Toxicol.* 29, 341-354.
- Rzagalinski B.A. and Strobl J.S. (2009). Cadmium-containing nanoparticles: perspectives on pharmacology and toxicology of quantum dots. *Toxicol. Appl. Pharmacol.* 238, 280-288.
- Roda E., Coccini T., Acerbi D., Barni S., Vaccarone R. and Manzo L. (2011). Comparative pulmonary toxicity assessment of pristine and functionalized Multi-Walled Carbon Nanotubes intratracheally instilled in rats: morphohistochemical evaluations. *Histol. Histopathol.* 26, 357-367.
- Rosenbruch M. (1992). Inhalation of amorphous silica: morphological and morphometric evaluation of lung associated lymph nodes in rats. *Exp. Toxicol. Pathol.* 44, 10-14.
- Saarikoski S.T., Wikman H.A-L., Smith G., Wolff H.J. and Husgafvel-Pursiainen K. (2005). Localization of cytochrome P450 CYP2S1 expression in human tissues by *in situ* hybridization and immunohistochemistry. *J. Histochem. Cytochem.* 53, 549-556.
- Saffiotti U. (1992). Lung cancer induction by crystalline silica. *Prog. Clin. Biol. Res.* 374, 51-69.
- Sayes C.M., Reed K.L. and Warheit D.B. (2007). Assessing toxicity of fine and nanoparticles: comparing *in vitro* measurements to *in vivo* pulmonary toxicity profiles. *Toxicol. Sci.* 97, 163-180.
- Shiozawa F., Kasama T., Yajima N., Odai T., Isozaki T., Matsunawa M., Yoda Y., Negishi M., Ide H. and Adachi M. (2004). Enhanced expression of interferon-inducible protein 10 associated with Th1 profiles of chemokine receptor in autoimmune pulmonary inflammation of MRL/lpr mice. *Arthritis Res. Ther.* 6, R78-R86.
- Slowing I.I., Vivero-Escoto J.L., Wu C.W. and Lin V.S. (2008). Mesoporous silica nanoparticles as controlled release drug delivery and gene transfection carriers. *Adv. Drug Deliv. Rev.* 60, 1278-1288.
- Song Y., Li X., Wang L., Rojanasakul Y., Castranova V., Li H. and Ma J. (2011). Nanomaterials in humans: Identification, characteristics, and potential damage. *Toxicol. Pathol.* 00, 1-9.
- Vallhov H., Qin J., Johansson S.M., Ahlborg N., Muhammed M.A., Scheynius A. and Gabrielsson S. (2006). The importance of an endotoxin-free environment during the production of nanoparticles used in medical applications. *Nano Lett.* 6, 1682-1686.
- Vivero-Escoto J.L., Slowing I.I., Trewyn B.G. and Lin V.S. (2010). Mesoporous silica nanoparticles for intracellular controlled drug delivery. *Small* 6, 1952-1967.
- Voit Fanucchi M., Murphy M.E., Buckpitt A.R., Philpot R.M. and Plopper C.G. (1997). Pulmonary cytochrome P450 monooxygenase and Clara cell differentiation in mice. *Am. J. Respir. Cell. Mol. Biol.* 17, 302-314.
- Waalkes M.P. (2003). Cadmium carcinogenesis. *Mutat. Res.* 533, 107-120.
- Wang J.J., Sanderson B.J. and Wang H. (2007). Cytotoxicity and genotoxicity of ultrafine crystalline SiO₂ particulate in cultured human lymphoblastoid cells. *Environ. Mol. Mutagen.* 48, 151-157.
- Weibel E.R. (1979). Stereological methods. Vol. 1: Practical methods for biological morphometry. Academic Press Inc. London.
- Willis B.C., Liebler J.M., Luby-Phelps K., Nicholson A.G., Crandall E.D., du Bois R.M. and Borok Z. (2005). Induction of epithelial-mesenchymal transition in alveolar epithelial cells by transforming growth factor-beta1: potential role in idiopathic pulmonary fibrosis. *Am. J. Pathol.* 166, 1321-1332.
- Yu M., Zheng X., Witschi H. and Pinkerton K.E. (2002). The role of interleukin-6 in pulmonary inflammation and injury induced by exposure to environmental air pollutants. *Toxicol. Sci.* 68, 488-497.
- Zhang Q., Kusaka Y., Zhu X., Sato K., Mo Y., Kluz T. and Donaldson K. (2003). Comparative toxicity of standard nickel and ultrafine nickel in lung after intratracheal instillation. *J. Occup. Health* 45, 23-30.